AIP Applied Physics Letters

Shape-adaptable hyperlens for acoustic magnifying imaging

Hongkuan Zhang, Xiaoming Zhou, and Gengkai Hu

Citation: Applied Physics Letters **109**, 224103 (2016); doi: 10.1063/1.4971364
View online: http://dx.doi.org/10.1063/1.4971364
View Table of Contents: http://scitation.aip.org/content/aip/journal/apl/109/22?ver=pdfcov
Published by the AIP Publishing

APPLIED PHYSICS LETTERS **109**, 224103 (2016)

Shape-adaptable hyperlens for acoustic magnifying imaging

Hongkuan Zhang, Xiaoming Zhou,[a] and Gengkai Hu
Key Laboratory of Dynamics and Control of Flight Vehicle, Ministry of Education and School of Aerospace Engineering, Beijing Institute of Technology, Beijing 100081, China

(Received 26 September 2016; accepted 21 November 2016; published online 2 December 2016)

Previous prototypes of acoustic hyperlens consist of rigid channels, which are unable to adapt in shape to the object under detection. We propose to overcome this limitation by employing soft plastic tubes that could guide acoustics with robustness against bending deformation. Based on the idea of soft-tube acoustics, acoustic magnifying hyperlens with planar input and output surfaces has been fabricated and validated experimentally. The shape-adaption capability of the soft-tube hyperlens is demonstrated by a controlled experiment, in which the magnifying super-resolution images remain stable when the lens input surface is curved. Our study suggests a feasible route toward constructing the flexible channel-structured acoustic metamaterials with the shape-adaption capability, opening then an additional degree of freedom for full control of sound. *Published by AIP Publishing.* [http://dx.doi.org/10.1063/1.4971364]

Metamaterial hyperlens has shown the ability to image objects with a resolution beyond the diffraction limit.[1,2] They can be achieved by the careful design upon nearly flat dispersions over a wide range of angular momentums. Evanescent waves with high angular momentum values can be therefore be converted into the propagating ones and transferred without decaying to the far side, contributing ultimately to the super-resolution acoustic images. In acoustics, the formation of the nearly flat dispersion relies on the anisotropic-mass effect, and it is also necessary to enable the mass component in the lens lateral direction extremely large. Following the above requirements, the near-field hyperlenses are usually constructed with a cluster of straight rigid channels,[3–5] which have been further filled by soft elastic layers[6–8] or corrugated[9] in order to lower the thickness-to-wavelength ratio.

The near-field hyperlenses refer to those without the magnifying effect, and therefore project the images in the near field only. The reason is that although converted to propagate within the lens, evanescent waves will be recovered when they are outside. On the contrary, the far-field magnifying hyperlens can permanently convert evanescent waves into propagating ones. They compress the tangential wave-vectors of evanescent waves into the propagating regime by enlarging the lateral size of the output surface with respect to the input side, so that the subwavelength images are magnified and become detectable in the far field.[10,11] By potentially combining the current far-field imaging systems, the magnifying hyperlens may become a promising super-resolution imaging device. In previous studies, the magnifying hyperlens consists in the straight rigid channels; they are in the cylindrical conformation,[12] and are difficult to adapt to the object shape under detection. In this work, we propose to construct a planar magnifying hyperlens with soft plastic tubes, which are flexible and easily deformed. The shape-adaption capability of the lens will be demonstrated by the experimental stable imaging against the lens deformation. The idea has been inspired by the physics discovered recently in extraordinary acoustic transmission for non-straight tubes. It has been observed that,[13] once acoustics are squeezed into a narrow channel, acoustic transmission can be insensitive to the non-straight, bended or coiled, geometry of the channel. It means that long-length channels can be bended or coiled into a tight space without remarkably altering the sound channeling effects. As a result, the coiling-up-space acoustic metamaterials with negative index,[14–16] and bending-channel acoustic metasurfaces[17–19] have been successfully realized.

The proposed magnifying hyperlens is made of the regular arrangement of soft Polyvinyl chloride (PVC) hollow tubes as shown in Fig. 1. The inner and outer diameters of each tube are, respectively, 0.8 cm and 1.2 cm. The tube length is chosen as 30 cm, which would determine the imaging frequency as explained later. The used PVC material has the mass density 1300 kg/m^3, Poisson's ratio 0.47, and a relatively low Young's modulus 30 MPa, which ensures the easy bending deformation of the tubes. The 2 mm-thick PMMA plates are used as the input and output surfaces of the hyperlens and set as being planar initially. Either plate is punched with 30 round holes, which are arranged in three rows and ten columns. The center-to-center distances of holes between adjacent rows are all 1.5 cm. The hole separation between columns is 2 cm on the input plate and 6 cm on the output plate; their ratio 6/2 = 3 defines the magnifying factor of this hyperlens. We then use soft tubes to connect holes perforated on the one plate to those with the same row and column numbers on the other plate. The distance between plates, defined as the thickness of the lens, is set as 23 cm. It is seen in Fig. 1 that soft tubes are able to deform adaptively in order for conforming to the planar boundaries of the hyperlens.

Acoustic transmission of the soft tube is evaluated by experimental measurement using the Brüel & Kjær 4206 impedance tube. Figure 2 shows transmission amplitudes of the soft plastic tube in the straight and deformed states, as well as a straight and stiffer PMMA tube (Young's modulus 2.3 GPa, Poisson's ratio 0.38, density 1200 kg/m^3 for PMMA material) of the same size. Note that the soft tube with the

[a]Author to whom correspondence should be addressed. Electronic mail: zhxming@bit.edu.cn

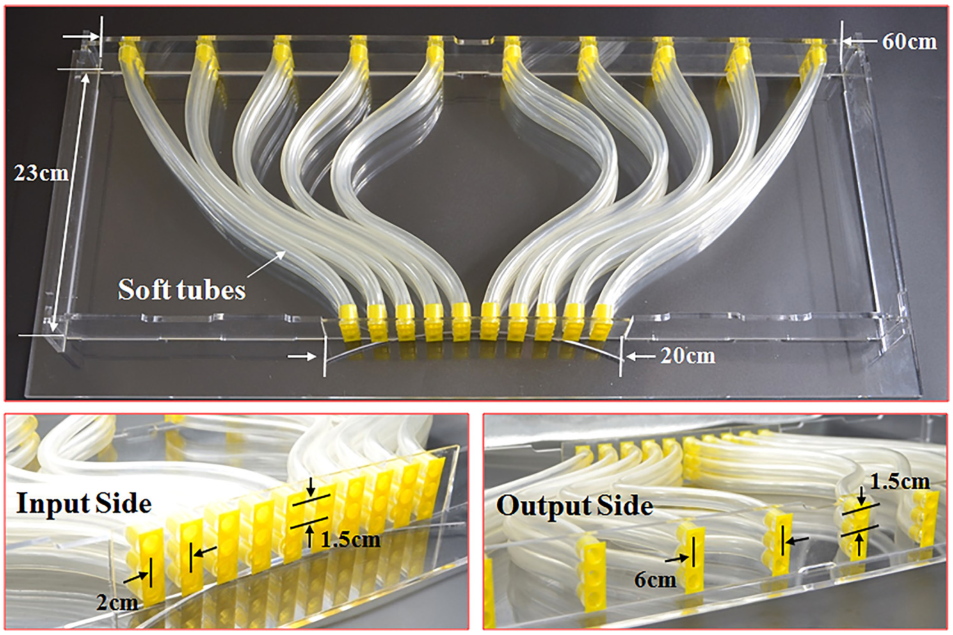

FIG. 1. Flexible acoustic magnifying hyperlens fabricated by soft plastic tubes.

biggest bending deformation observed in the structured hyperlens is examined. Excellent agreement of transmissions between the straight and curved soft tubes can be observed, verifying the robustness of acoustic channeling against the tube's bending deformation. Compared to the stiff tube, transmission amplitudes across soft tube have been lowered near peak transmission frequencies, apparently because of the greater viscous damping in the plastic materials. The comparison results lead to the other conclusion important to the imaging effect in that the nontrivial damping would not alter the peak transmission frequencies. As a concluding remark, the only price for using soft materials to design acoustic hyperlens is the lowered transmission due to the inevitable damping, which is not detrimental to the imaging, but can be solved by increasing the signal-to-noise ratio in practice. In the following, we will develop an analytic model based on the straight-channel unit cell in order to define the imaging frequency of the hyperlens.

The proposed hyperlens is designed in a manner to confine acoustic energy in the narrow tubes only, instead of in the region between tubes. It means that acoustic characteristics of the hyperlens are irrelevant to the distance between

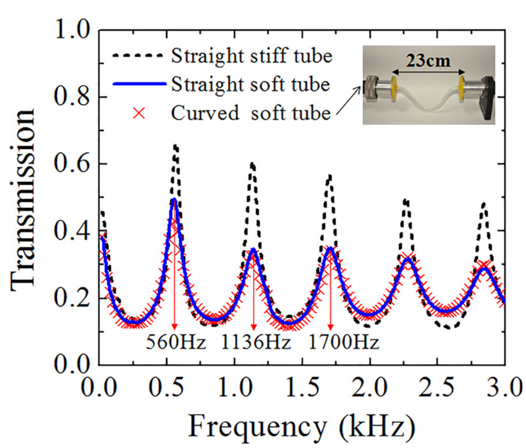

FIG. 2. Acoustic transmission measured for straight and curved soft PVC tubes as well as for a straight stiff PMMA tube for comparison.

tubes. Hence the bundle of deformed tubes can be treated as an effectively homogeneous medium, even though the distance between nearby tubes changes dramatically along the thickness direction of the lens. Figure 3 shows one channel cell of the magnifying hyperlens, which differs from a near-field hyperlens[9] in that the periodicity of holes on the output region has been enlarged $a_1/a_0 > 1$. Assume that d, a_0, and a_1 are all smaller than the wavelength; the influence of the discretization in the structured hyperlens becomes very small. Then an analytic homogenization model can be established to characterize the acoustic transportation by the channel structure. Above assumption has ensured that the narrow channels support the dominate zeroth-order mode. Therefore, the tube of the diameter d can be represented effectively by an acoustic fluid with anisotropic mass density $\tilde{\boldsymbol{\rho}} = \mathrm{diag}[\rho, \infty]$, $\rho = 4\rho_0 a_0^2/(\pi d^2)$, where ρ_0 and c_0 are, respectively, the mass density and sound velocity of the background medium, and the infinite mass along the interface direction arises from the vanishing acoustic interaction among tubes. The transmitted region with the periodicity a_1 is equivalent to an acoustic media with the scalar density $\rho_1 = \rho_0 a_0/a_1$. In all regions, the sound velocity c_0 remains unchanged. It is known that the dispersion equation for a homogenized anisotropic-mass acoustic medium is written as $k_x^2/\rho_x + k_y^2/\rho_y = \omega^2/\kappa$. Infinite ρ_y for the present hyperlens ensures the nearly flat dispersion curve with respect to the parallel wave vector k_y in either propagating or evanescent wavenumber space, which demonstrates the origin of the hyperlens.

According to the effective-medium model, the transmission coefficient for the channel of length L can be derived as

$$T(\omega, k_y) = \frac{2z_1}{(z_0 + z_1)\cos(k_0 L) - i\left[\rho c_0 + z_0 z_1/(\rho c_0)\right]\sin(k_0 L)}, \tag{1}$$

where $z_0 = \rho_0\omega/\sqrt{k_0^2 - k_y^2}$ and $z_1 = \rho_1\omega/\sqrt{k_0^2 - k_y^2}$. Consider first $a_1 = a_0$, which refers to the case of a near-field hyperlens. In order for the complete transmission $T = 1$ for any k_y, it is necessary to let $\sin(k_0 L) = 0$. This results in

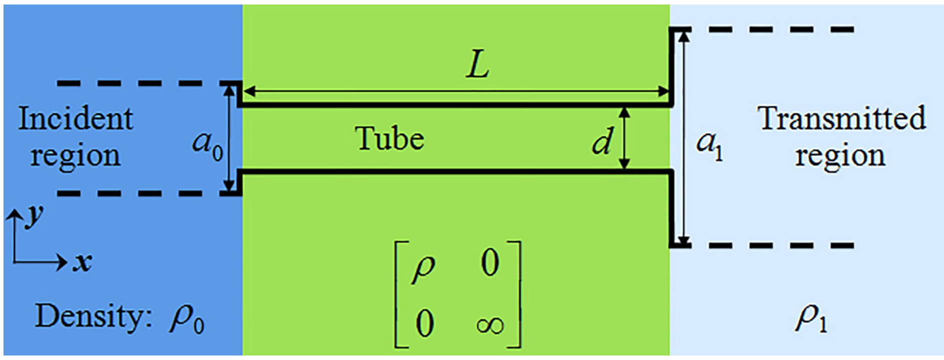

FIG. 3. Analytic modeling of one channel cell of the magnifying hyperlens, where the periodicity a_1 on the output side is bigger than a_0 on the input side in order to achieve the magnification effect.

the well-known Fabry-Pérot resonant condition that defines the imaging frequency as $f = n\frac{c_0}{2L}$ where n is an integer number. For the magnifying hyperlens with $a_1 > a_0$, the Fabry-Pérot resonance still provides a satisfactory condition to achieve the k_y-independent constant transmission $T = 2a_0/(a_0 + a_1)$. It can be seen that the transmission T will never reach unity as long as $a_1 > a_0$ is pursued for the magnifying effect. As a concluding remark, the reflection by the tube structure is inevitable due to either the existence of the small inlets and large reflectors between nearby tubes or the impedance mismatching because of $a_1 > a_0$. However, it is worth to stress that the lowered transmission would not alter the fact of the same transmission for all tubes, which is the most important condition to construct successively an acoustic hyperlens. This condition means that evanescent waves will be equally transmitted so that the subwavelength image magnified by the hyperlens will not be distorted. In the following, we will experimentally demonstrate that acoustic magnifying imaging can indeed be achieved even though there is no complete acoustic transmission across the tube. In our samples, the tube length is $L = 30$ cm; the first three resonant frequencies are found from Eq. (1) to be 567 Hz, 1133 Hz, and 1700 Hz, respectively. Notice that $\rho_0 = 1.25\,\text{kg/m}^3$ and $c_0 = 340$ m/s have been reasonably taken for the air. It is seen from Fig. 2 that theoretical predictions coincide very well with the measured peak transmission frequencies. In our experiment, the imaging frequency is chosen as the 3rd resonant frequency 1700 Hz for a compromise between the experimental measurement area and the lens size to wavelength ratio.

Figure 4(a) shows the established acoustic 2D scanning system[7] with an effective scanning area $30 \times 60\,\text{cm}^2$, which is employed here to measure both acoustic amplitudes and phases responded by the hyperlens. A dual source with the separation 6.67 cm is used to represent the defects to be magnified; it is created by a U-shape splitter with the input side connecting to a loudspeaker. Note that the center-to-center distance 6.67 cm is the one-third wavelength in air corresponding to the frequency 1700 Hz of operation. We have first measured the acoustic radiation fields emitted by this subwavelength "defects" (dual source) without being magnified by the hyperlens as shown in Fig. 4(b); the resultant fields look like the ones launched by a single source. This can be attributed to the subwavelength nature of the dual source, explaining why they cannot be distinguished from the far field. When the magnified hyperlens is placed at a distance of 2 mm in front of the dual source, the measured acoustic fields [Fig. 4(c)] show the strong wave interferences as a result of the magnifying effect. A comparable numerical simulation is also conducted [Fig. 4(d)], which repeats the experimental results. We will demonstrate below by numerical simulation that acoustic fields shown in Figs. 4(c) and 4(d) are indeed the magnified images of the subwavelength dual source.

In the simulation, either one of dual outputs of the experimental U-shape splitter can be modeled by a point source, since the output's aperture size is in the deep-subwavelength scale compared to the operating wavelength. The pressure distribution in the line locating 2 mm (same to the experimental

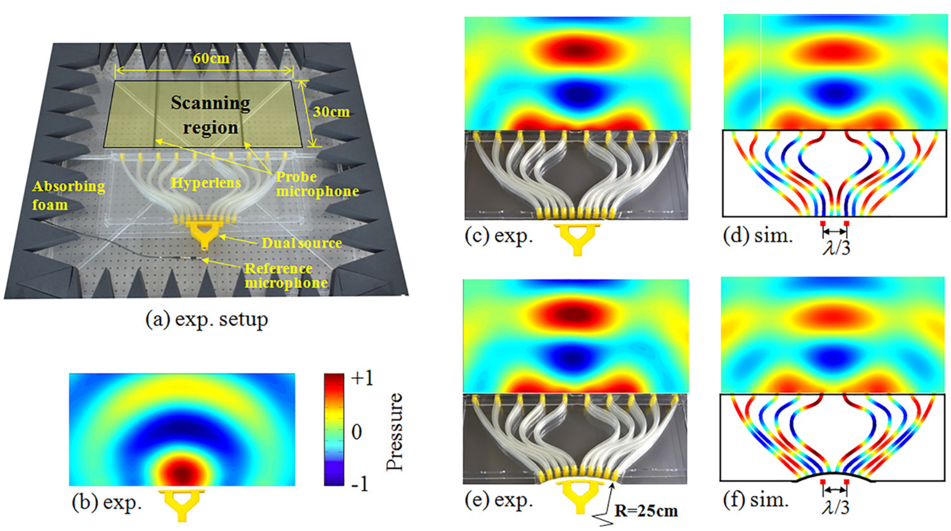

FIG. 4. (a) Acoustic 2D scanning system used to experimentally characterize the fabricated acoustic hyperlens; (b) measured acoustic fields radiated from dual sources with the subwavelength separation $\lambda/3$; acoustic fields measured above the soft-tube hyperlens with the planar input surface (c) and curved input surface having the curvature radius 25 cm (e); (d) and (f) simulation results corresponding, respectively, to (c) and (e).

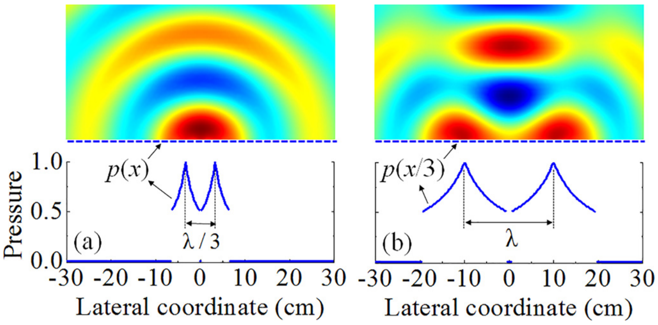

FIG. 5. (a) The pressure distribution $p(x)$ loaded on the lens input by the simulated dual source and their projected acoustic fields, which show the single-source acoustic features as similar to experimental results [Fig. 4(b)]. (b) The pressure distribution $p(x/3)$ obtained by magnifying $p(x)$ three times along the lateral direction and their projected acoustic fields, which are in excellent agreement to measured acoustic fields [Fig. 4(c)], firmly validating the $\times 3$ magnifying capability of the soft-tube hyperlens.

environment) away from a point source can be readily computed, which we consider as the pressures loading on the input surface of the hyperlens. The resultant pressures loaded upon the lens input by the dual source are denoted by $p(x)$ and shown in Fig. 5(a), where the pressure distribution has been normalized to its maximum value and in addition only lateral regions with pressures beyond the half maximum are retained for simplification. It can be seen that acoustic fields projected by this simulated dual source exhibit the single-source acoustic features as similar to experimental results [Fig. 4(b)]. The proposed hyperlens functions in a manner that the pressure distribution $p(x)$ in Fig. 5(a) is to be laterally magnified three times, resulting in a new pressure distribution denoted by $p(x/3)$, which together with their projected acoustic fields are shown in Fig. 5(b). Excellent agreement between measured acoustic fields [Fig. 4(c)] and this simulation result can be found, which then firmly validates the $\times 3$ magnifying capability of the soft-tube hyperlens.

We further announce that the proposed flexible hyperlens is able to conform adaptively to the uneven profile of the object under detection. As an example of verification, the U-shaped dual source is now replaced by the one having the circular output profile with the curvature radius 25 cm. Figure 4(e) shows the acoustic fields measured in front of the hyperlens that has the planar output, while its input surface is curved with the same circular profile as the source side. It is clearly seen that the magnifying images of the dual source remains stable against the curved deformation of the soft-tube lens. Figure 4(f) shows the comparative simulation results, verifying again the shape-conformation capability of the soft hyperlens.

In our experiment, we have also verified that the damping of soft tubes has a minor influence on the imaging effect, although it reduces the sound transmission amplitude near resonant frequencies. The reason of the result is that the hyperlens imaging relies mainly on the uniform transmission over the entire wave-vector space, instead of achieving the maximum transmission permitted by the lens structure. Except around the resonant frequencies, energy absorption due to damping becomes minor so that the soft tube is not acoustically inferior to the stiff channel, as seen in Fig. 2. Hence, soft acoustic tubes may be potentially used to facilitate the fabrication of non-resonant channel-structured metamaterials[14] and metasurfaces.[17] On the other hand, the damping may become advantageous when soft tubes are used to facilitate the channel-structured sound absorbing devices.[20,21] Note finally that acoustic controlling devices constructed with soft tubes are potentially robust against the structure deformation.

As a summary, we have reported that soft plastic tubes can be efficient channeling structures that transmit acoustics with the robustness against bending deformation. The idea of soft-tube acoustics has helped realizing a planar magnifying hyperlens capable of easy deformation necessary for shape conformation to the object under detection. These unique features have been firmly verified by our experiments. The proposed soft hyperlens can be regarded as an improved version based on the previous prototype that has to be in cylindrical conformation by using straight rigid tubes.[12] It is worth to stress that soft-tube acoustics may be further extended to improve a wide variety of channel-structured acoustic metamaterials and metasurfaces by equipping them with flexible and adaptive capabilities, opening then an additional degree of freedom toward full control of sound.

This work has been supported by the National Natural Science Foundation of China (Grant Nos. 11521062, 11572039, and 11622215), and 111 project (B16003).

[1]D. Lu and Z. Liu, Nat. Commun. **3**, 1205 (2012).
[2]X. Zhang and Z. Liu, Nat. Mater. **7**(6), 435–441 (2008).
[3]J. Zhu, J. Christensen, J. Jung, L. Martin-Moreno, X. Yin, L. Fok, X. Zhang, and F. J. Garcia-Vidal, Nat. Phys. **7**(1), 52–55 (2011).
[4]H. Jia, M. Ke, R. Hao, Y. Ye, F. Liu, and Z. Liu, Appl. Phys. Lett. **97**(17), 173507 (2010).
[5]C. Shen, Y. Xie, N. Sui, W. Wang, S. A. Cummer, and Y. Jing, Phys. Rev. Lett. **115**(25), 254301 (2015).
[6]X. Zhou and G. Hu, Appl. Phys. Lett. **98**(26), 263510 (2011).
[7]X. Xu, P. Li, X. Zhou, and G. Hu, EPL **109**(2), 28001 (2015).
[8]J. Christensen and F. J. García de Abajo, Appl. Phys. Lett. **97**(16), 164103 (2010).
[9]H. Su, X. Zhou, X. Xu, and G. Hu, J. Acoust. Soc. Am. **135**(4), 1686–1691 (2014).
[10]Z. Liang and J. Li, AIP Adv. **1**(4), 041503 (2011).
[11]R. Zhu, Y. Y. Chen, Y. S. Wang, G. K. Hu, and G. L. Huang, J. Acoust. Soc. Am. **139**(6), 3303–3310 (2016).
[12]J. Li, L. Fok, X. Yin, G. Bartal, and X. Zhang, Nat. Mater. **8**(12), 931–934 (2009).
[13]R. Fleury and A. Alù, Phys. Rev. Lett. **111**(5), 055501 (2013).
[14]Z. Liang and J. Li, Phys. Rev. Lett. **108**(11), 114301 (2012).
[15]Y. Xie, B.-I. Popa, L. Zigoneanu, and S. A. Cummer, Phys. Rev. Lett. **110**(17), 175501 (2013).
[16]T. Frenzel, J. D. Brehm, T. Bueckmann, R. Schittny, M. Kadic, and M. Wegener, Appl. Phys. Lett. **103**(6), 061907 (2013).
[17]Y. Xie, W. Wang, H. Chen, A. Konneker, B.-I. Popa, and S. A. Cummer, Nat. Commun. **5**, 5553 (2014).
[18]K. Tang, C. Qiu, M. Ke, J. Lu, Y. Ye, and Z. Liu, Sci. Rep. **4**, 6517 (2014).
[19]Y. Li, X. Jiang, R.-Q. Li, B. Liang, X.-Y. Zou, L.-L. Yin, and J.-C. Cheng, Phys. Rev. Appl. **2**(6), 064002 (2014).
[20]X. Cai, Q. Guo, G. Hu, and J. Yang, Appl. Phys. Lett. **105**(12), 121901 (2014).
[21]Y. Li and B. M. Assouar, Appl. Phys. Lett. **108**(6), 063502 (2016).